The Preparation, Structure, and Conductivity of Scandium-Substituted NASICONs

M. A. SUBRAMANIAN, P. R. RUDOLF, AND A. CLEARFIELD

Department of Chemistry, Texas A&M University,
College Station, Texas 77843

A series of NASICON type compounds was prepared in which Sc(III) partially replaced Zr(IV). By simultaneously correlating the extent of this substitution with the amount of Si(IV) replacement of P(V) it was possible to obtain a series with a constant amount (3 mole) of sodium ion. All of the rhombohedral members of this series exhibited similar conductivities and activation energies over the temperature range 30–350°C. Transformation to the monoclinic phase occurred at a composition of $Na_3Sc_{0.5}Zr_{1.5}Si_{1.5}P_{1.5}O_{12}$ and was accompanied by a threefold increase in conductivity. Activation energies of the monoclinic (room temperature) phases in the temperature range 200–300°C were 0.2–0.23 eV. Crystal structures of the rhombohedral phase of composition $Na_3ScZrSiP_2O_{12}$ and the monoclinic phase, $Na_3Sc_{0.5}Zr_{1.5}Si_{1.5}P_{1.5}O_{12}$, were carried out by Rietveld refinement of their X-ray powder patterns. The structures confirmed those presented by Hong, and also confirmed the stoichiometry of these phases as evidenced from site occupancy refinement. These results were compared with the structure of a nonstoichiometric phase, $Na_{3.20}Zr_{1.68}Si_{1.84}P_{1.16}O_{11.54}$, prepared by a hydrothermal route. In the latter case it was shown that the low Zr content is due to Na^+ substitution for Zr^{4+}. No such substitution occurred in the scandium containing phases, and it is suggested that when Sc^{3+} substitution for zirconium takes place it prevents the sodium ion from occupying these sites. © 1985 Academic Press, Inc.

Introduction

The discovery of NASICON (*1, 2*) represented an important development in the field of solid electrolytes because it demonstrated that a three-dimensional framework structure was capable of supporting Na^+ conductivities comparable to that of β-alumina. However, a number of workers (*3–6*) have reported difficulty in synthesizing the superion conducting monoclinic compositions by high-temperature solid-state reaction. In most cases it was found that some ZrO_2 remains unreacted; but other phases, probably phosphates, have also been ob-

served (*7*). We have subsequently prepared monoclinic NASICON by a hydrothermal route (*8, 9*), and found this product to be free of contaminate crystalline phases. Fluorescence analysis, for the elements, showed that the composition is close to $Na_{3.3}Zr_{1.65}Si_{1.9}P_{1.1}O_{11.5}$. However, it is possible that the presence of glassy or amorphous material may account for the nonstoichiometry. Glass inclusions may be detected by electron microscopy (*10*), but amorphous phases are more difficult to identify. Electron microprobe analysis is effective if the second phase is a stable crystalline one such as ZrO_2 or $ZrSiO_4$.

However, we have observed that NASI-CON is not stable in the electron beam. The surface becomes negatively charged, and sodium metal bubbles out of the crystallites converting them to amorphous material.

Engell *et al.* (*10*), used a sol–gel technique to prepare stoichiometric phases which corresponded to the compositional formula proposed by Hong, $Na_{1+x}Zr_2Si_x$ $P_{3-x}O_{12}$. Thus, the question arises as to the correct representation for the NASICON family, and it has been suggested (*11*) that both stoichiometric and nonstoichiometric compositions exist. Obviously a structural technique independent of the method of preparation is required to settle this question. Preliminary studies on single crystals (*12, 13*) have indeed shown that nonstoichiometry does exist. Because the crystals are flux-grown it is possible that elements of the flux are introduced into the crystals. We have therefore undertaken a thorough examination of various NASICONS by both X-ray and neutron powder diffraction techniques. In this paper we report results obtained by partially substituting Sc^{3+} for Zr^{4+} because in this system stoichiometric compositions are routinely obtained.

Experimental

1. Synthesis and Characterization

The starting materials used were of high purity: ZrO_2 (99.99%, Aldrich); SiO_2 (99.99%, Alfa); Sc_2O_3 (99.999%, Aldrich); and Na_3PO_4 (99.9%, Fisher). ZrP_2O_7 was prepared by heating α-zirconium phosphate, $Zr(HPO_4)_2 \cdot H_2O$ (prepared from Hf-free $ZrOCl_2 \cdot 8H_2O$, spec. pure) at 900°C for 6 hr (*14*). Exact mole ratios of the starting materials were weighed out and ground together in an agate mortar until thoroughly blended. The entire solid was added to a platinum tube (4-mm o.d.) and sealed. The tube was slowly heated to 900°C for 4 hr and again at 1150–1200°C for 20 hr. The tubes were weighed before and after heat-

ing to ensure that no weight loss occurred. Samples were then reground and reheated to obtain single phases.

X-ray diffraction powder patterns were recorded with a Seifert–Scintag PADII computer automated powder diffractometer using $CuK\alpha$ radiation ($\lambda = 1.5418$ deg) by step-scanning the sample at 0.02 deg/5 sec. The position of each peak was determined by peak search programs. Accurate lattice parameters were calculated by using the least-squares program LSUCRE (*15*). Silicon powder (NBS–SRM 640, $a = 5.43088$ Å) was used as an internal standard.

2. Conductivity Measurements

Ionic conductivity measurements were performed on the samples in the form of sintered pellets by the complex impedance method (*16*). The pellets (8-mm diam and 2–3 mm thick) were made at room temperature in an evacuative die at 10 tons/sq. in. and the pellets were sintered at 1150–1200°C for 24 hr in a closed platinum crucible. These pressed and sintered pellets were polished with 400-grade emergy paper and the faces were coated with conductive platinum paint (Engelhard 6042) and heated at 600°C to evaporate the solvent. For conductivity measurements the pellets were sandwiched between two platinum plates which were spring-loaded to ensure good electrolyte/electrode contact. Temperature control was effected with a Barber–Coleman controller (Model 520) and Hewlett–Packard (HP) 59501B programmer. The temperature was measured with an HP 3421 Data Acquisition Unit with internal temperature calibration. Impedance measurements were performed in the frequency region 5 Hz to 13 MHz using an HP 4192A impedance analyzer, and when required to 108 MHz with an HP 4815 unit. Twenty experimental points were taken for each decade of frequency using a log sweep mode. The temperature range was 30–350°C. All

TABLE I

UNIT CELL DIMENSIONS AND CONDUCTIVITY DATA FOR SCANDIUM–SUBSTITUTED NASICONS

| Compound | Structure | Lattice parameters | | | | $\sigma_{300°C}$ (ohm^{-1} cm^{-1}) | Ea[a] (eV) |
		a (Å)	b (Å)	c (Å)	β (°)		
$Na_3(Sc_{1.5}Zr_{0.5})Si_{0.5}P_{2.5}O_{12}$	R[b]	8.937		22.447		0.029	0.33
$Na_3(Sc_{1.2}Zr_{0.8})Si_{0.8}P_{2.2}O_{12}$	R	8.963		22.541		—	—
$Na_3(ScZr)SiP_2O_{12}$	R	8.985		22.612		0.031	0.31
$Na_3(Sc_{0.8}Zr_{1.2})Si_{1.2}P_{1.8}O_{12}$	R	8.999		22.717		0.029	0.32
$Na_3(Sc_{0.5}Zr_{1.5})Si_{1.5}P_{1.5}O_{12}$	M	15.616	9.019	9.184	123.92	0.107	0.23
$Na_3(Sc_{0.2}Zr_{1.8})Si_{1.8}P_{1.2}O_{12}$	M	15.632	9.031	9.220	123.98	0.120	0.21
$Na_{3.3}(Sc_{0.3}Zr_{1.7})Si_2PO_{12}$	M	15.644	9.054	9.215	124.0	0.179	0.20
$Na_{3.5}(Sc_{0.5}Zr_{1.5})Si_2PO_{12}$	R	9.095		22.548		0.100	0.32
$Na_{2.5}(Sc_{0.2}Zr_{1.8})Si_{1.3}P_{1.7}O_{12}$	R	8.990		22.878		0.045	0.30
$Na_{2.7}(Sc_{0.2}Zr_{1.8})Si_{1.5}P_{1.5}O_{12}$	R–M[c]	9.021		22.651		0.081	0.28
$Na_2(ZrSc)P_3O_{12}$	R	8.861		22.518		0.009	0.40

[a] Ea values for monoclinic phases are for the temperature range 200–300°C.

[b] R = rhombohedral, M = monoclinic.

[c] Borderline monoclinic.

the measuring instruments and temperature controls were interfaced to an HP 8916 desk top computer. The impedance plots and the least-squares fitting of conductivity data were done using computer programs (17). Both cell and furnaces were grounded to avoid stray a.c. fields.

3. Crystal Structure Determination

Two of the scandium-containing phases, $Na_3(ScZr)SiP_2O_{12}$ and $Na_3Sc_{0.5}Zr_{1.5}Si_{1.5}P_{1.5}O_{12}$, were chosen for X-ray structure studies. The former is rhombohedral and the latter monoclinic at room temperature. Powder data were collected by step-scanning (0.02° in 2θ and 72 sec/step) in the range of 10–80° 2θ. Data reduction and mathematical $K\alpha_2$ stripping were accomplished as described previously (18). Rietveld refinement was carried out with the XRS–82 series of programs (19) modified for use on a VAX 11/780 computer (18). The starting model for the rhombohedral phase was that provided by Kohler and Schulz (13) for a single crystal of approximate composition $Na_{3.1}Zr_{1.78}Si_{1.24}P_{1.76}O_{12}$. No sodium atoms were included in the initial model and Zr/Sc and Si/P were assumed

to be statistically distributed in their positional sites at full occupancy. Refinement proceeded smoothly to convergence with isotropic temperature factors. A difference Fourier then revealed the positions of the sodium ions in Type I and two-thirds of the Type II cavities. The refinement was again carried to convergence and then the Na^+ site occupancies were refined. It was found that Type I cavities contained 0.85 Na^+ while the Type II cavities contained 2.15. At this stage anisotropic thermal parameters were introduced and refined. In the final stages all parameters were refined to convergence.

For the monoclinic compound the starting model was that proposed by Hong (2), and refinement was carried out in the same way as described above.

Results

Unit cell parameters and conductivity data for the scandium-substituted NASICONs are given in Table I. In one series of samples the sodium content was kept constant at 3.0 by correlated adjustments of the Sc^{3+} and Si^{4+} contents. In this series the
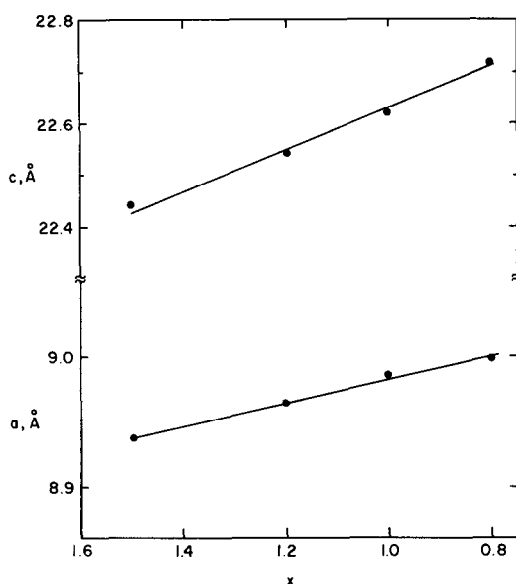
FIG. 1. Variation of hexagonal unit cell parameters as a function of x in $Na_3Sc_xZr_{2-x}Si_{2-x}P_{1+x}O_{12}$.

unit cell parameters increased linearly as the silicon content increased (Fig. 1). However, for the rhombohedral members of this series, the conductivity remained constant with increase in Si content as did the activation energy. In contrast, a dramatic increase in conductivity was observed for the monoclinic phases. The large increase must be structurally defined as the sodium ion content was held constant.

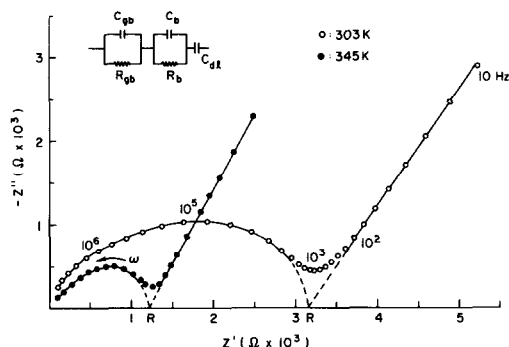A typical impedance plot is shown in Fig. 2. Similar plots were obtained for all the

samples. The plots showed two characteristic features commonly observed (3, 20, 21) for ceramic solid electrolytes when measurements are made with blocking electrodes. The first appears at low frequencies and is a straight line associated with series capacitance of the blocking electrodes. The second feature appears at higher frequencies and is a distorted semicircle due to resistive and capacitive (RC) components of the solid electrolyte. The distortion is due to overlapping of two semicircles associated with grains and intergrain boundaries within the bulk of the solid electrolytes. It arises when the difference between the RC constants (or relaxation times) of the grains and intergrain boundaries is small so that both contribute to Z'' at some frequencies (3). Kleitz and Kennedy (22) have shown that significant overlap occurs when relaxation times of two components differ by less than a factor of 100. In such cases the accu-

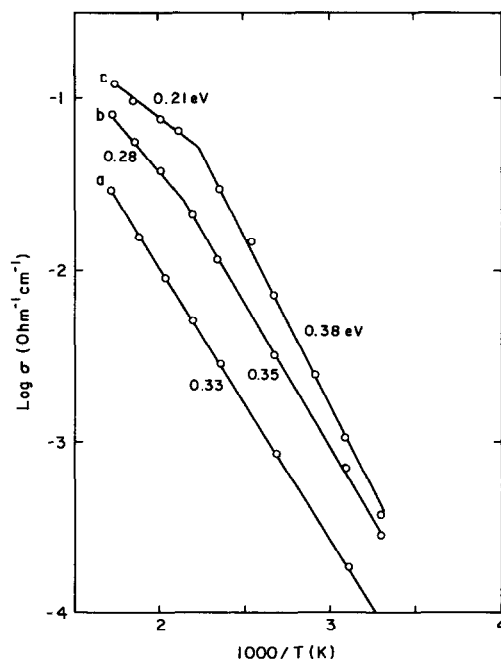FIG. 2. Complex impedance plane diagrams for Na_3 $ScZrSiP_2O_{12}$ at two different temperatures. Inset shows the equivalent circuit.

FIG. 3. Arrhenius plots of log conductivity vs reciprocal temperatures for scandium-substituted NASICONs: (a) rhombohedral $Na_3Sc_{1.5}Zr_{0.5}Si_{0.5}P_{1.5}O_{12}$; (b) monoclinic $Na_{2.7}Sc_{0.2}Zr_{1.8}Si_{1.5}P_{1.5}O_{12}$; (c) monoclinic $Na_3Sc_{0.2}Zr_{1.8}Si_{1.8}P_{1.2}O_{12}$.

rate calculation of intermediate resistance values becomes difficult. The semicircles become more regular with increase in temperature and eventually ($\approx 300°C$) only the straight line portion was obtained as has been observed for other highly conducting solid electrolytes $(4, 21)$. The total or bulk resistance (R) was taken to be the value of Z' at the intersection of the extrapolated linear portion with the Z' axis.

Conductivities were calculated as

$$\sigma = d/AR \qquad (1)$$

where d is the thickness of the disk and A its area. Bulk densities of the sintered disks were normally 85–90% of theoretical.

Figure 3 shows Arrhenius plots, one for a rhombohedral phase and another for a monoclinic phase, both containing 3 mole Na^+ per formula weight, and a third composition which could be indexed as either rhombohedral or monoclinic. There is no change in slope of the conductivity plot for the rhombohedral phase, but a fairly dramatic one for the monoclinic phase. We interpret this change as due to a phase transformation from monoclinic to rhombohedral, a transformation previously reported for NASICON $(4, 23)$. The very slight change in slope for curve 2 indicates that this phase, of composition $Na_{2.7}(Sc_{0.2}Zr_{1.8})Si_{1.5}P_{1.5}O_{12}$, is probably monoclinic at room temperature. Considering then only those phases that are monoclinic at room temperature, we observe a steady increase

in conductivity at 300°C with increased Si or Na^+ content. A maximim conductivity is attained with the composition of $Na_{3.3}(Sc_{0.3}Zr_{1.7})Si_2PO_{12}$ and a further increase in sodium content results in a decrease in conductivity. However, this decrease is accompanied by a reversion to a rhombohedral structure. Activation energies in Table I parallel those reported for non-scandium-containing NASICONs (4).

Structural Results

Crystallographic data for the rhombohedral phase are given in Tables II–IV while the data for the monoclinic phase are col-

TABLE II

CRYSTAL STRUCTURE DATA FOR SCANDIUM-SUBSTITUTED NASICONs; CRYSTALLOGRAPHIC DATA FOR RHOMBOHEDRAL $Na_3ScZrSiP_2O_{12}$

Space group	$R\bar{3}c$	
Hexagonal cell parameters		
a	8.9848(1) Å	
c	22.6113(2) Å	
Cell volume	1580.8 Å³	
Z	6	
Step scan data limits	$(2\theta)13–79.8°$	
No. of steps	3060	
Step width	0.02°	
Step time	72 sec	
No. of contributing reflections	95	
No. of parameters	97	
R values	Observed	Statistically calculated
$R_F = (\Sigma||I_o^{1/2}| - |I_c^{1/2}|)/\Sigma|I_o^{1/2}|$	0.052	0.038
$R_I = (\Sigma||I_o| - |I_c||)/\Sigma|I_o|$	0.076	0.078
$R_{wp} = \{\Sigma w_i[y_{io} - (y_{ic}/c)]^2/\Sigma w_i y_{io}^2\}^{1/2}$	0.132	0.124

TABLE III

CRYSTAL STRUCTURE DATA FOR SCANDIUM-SUBSTITUTED NASICONs; POSITIONAL AND THERMAL PARAMETERS FOR RHOMBOHEDRAL $Na_3ScZrSiP_2O_{12}$

Atom	x	y	z	Occupancy	u_{11}	u_{22}	u_{33}	u_{12}	u_{13}	u_{23}
Zr	0.0	0.0	0.1487(1)	0.5	0.00386	0.00386	0.02069	0.00193	0.0	0.0
Sc	0.0	0.0	0.1487(1)	0.5	0.00386	0.00386	0.02069	0.00193	0.0	0.0
Si	0.2954(18)	0.0	0.25	0.667	0.01019	0.01557	0.01263	0.00779	−0.00027	−0.0005
P	0.2954(18)	0.0	0.25	0.333	0.01019	0.01557	0.01263	0.00779	−0.00027	−0.0005
O1	0.1850(25)	−0.0263(30)	0.1954(10)	1.0	0.00990	0.01479	0.04231	0.00976	0.00659	0.0038
O2	0.1914(22)	0.1647(27)	0.0910(10)	1.0	0.00990	0.01479	0.04231	0.00976	0.00659	0.0038
Na1	0.0	0.0	0.0	0.854	0.29106	0.29106	0.04749	0.14553	0.0	0.0
Na2	0.6318	0.0	0.25	0.694	0.0300	0.02630	0.2235	0.01315	0.03742	0.07483

TABLE IV

CRYSTAL STRUCTURE DATA FOR
SCANDIUM-SUBSTITUTED NASICONS; BOND
LENGTHS AND ANGLES FOR RHOMBOHEDRAL
$Na_3ScZrSiP_2O_{12}$

Atoms	Bond length (Å)	Bond angle (deg)
Zr–O (ave)[a]	2.078(3)	
$\begin{Bmatrix} Si\text{–}O \\ P\text{–}O \end{Bmatrix}$ (ave)	1.552(26)	
Na1–O2	2.614(20)	
Na1–Na2	3.478(30)	
O–Zr–O (ave)		89.8(13)
O–P–O (ave)		109.9(7)
Zr–O–P (ave)		150(3)

[a] esd's are calculated as

$$[\Sigma_{i=1}^{N}|(\text{ave} - \text{obs}_i)^2|/N(N - 1)]^{1/2}.$$

lected in Tables V–VII. ORTEP drawings (*24*) of portions of the structures are given in Figs. 4 and 5. In essence the structures put forward previously (*2, 25, 26*) are confirmed. However, it should be noted that in the rhombohedral structure, the sodium ions in Type I cavities have an almost isotropic motion while those in Type II cavities have a highly anisotropic vibrational mo-
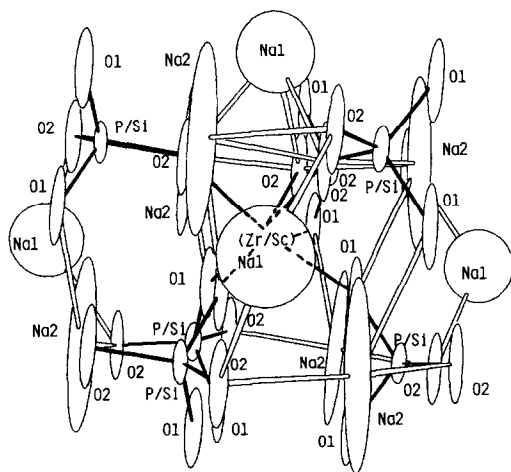

FIG. 5. An ORTEP representation of a portion of the $Na_3Sc_{0.5}Zr_{1.5}Si_{1.5}P_{1.5}O_{12}$ structure. The thermal ellipsoids are at the 10% probability level.

tion. The coordination about Na1 is a trigonal antiprism of O2 atoms as shown in Fig. 6. In this figure the *c* axis passes through the centers of the O2 triangles and the vibration of Na1 is directed almost perpendicular to the *c* axis and toward the Na2 sites. This is very similar to what was observed by Kohler and Schulz (*13*) in a single

FIG. 4. An ORTEP representation of a portion of the $Na_3ScZrSiP_2O_{12}$ structure. The thermal ellipsoids are at the 20% probability level.

TABLE V

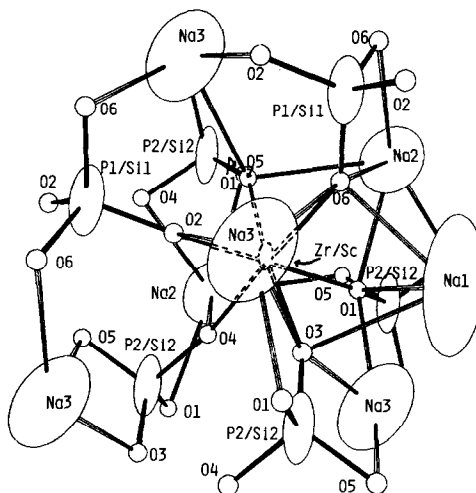CRYSTAL STRUCTURE DATA FOR
SCANDIUM-SUBSTITUTED NASICONS;
CRYSTALLOGRAPHIC DATA FOR MONOCLINIC
$Na_3Zr_{1.5}Sc_{0.5}P_{1.5}Si_{1.5}O_{12}$

Space group	$C2/c$	
a	15.6160(2)	
b	9.0188(1)	
c	9.1841(1)	
β	123.92(1)	
Z	4	
Refinement from	13–75°2θ	
No. of steps	2795	
Step width	0.02°2θ	
Step time	72 sec	
No. of contributing reflections	248	
No. of parameters (total)	151	
No. of geometric restrictions	35	
R values	Observed	Statistically calculated
$R_{wp} = \{\Sigma w_i[y_{io} - (y_{ic}/c)]^2/\Sigma w_i y_{io}^2\}^{1/2}$	0.142	(0.118)
$R_F = (\Sigma\||I_o^{1/2}| - |I_c^{1/2}\|)/\Sigma|I_o^{1/2}|$	0.083	(0.038)
$R_I = (\Sigma\||I_o| - |I_c\|)/\Sigma|I_o|$	0.063	(0.075)

TABLE VI

Crystal Structure Data for Scandium-Substituted NASICONs; Positional and Thermal Parameters for Monoclinic $Na_3Zr_{1.5}Sc_{0.5}P_{1.5}Si_{1.5}O_{12}$

Atom	x	y	z	Occupancy	u_{11}	u_{22}	u_{33}	u_{12}	u_{13}	u_{23}
Zr	0.1010(7)	0.2503(20)	0.0554(9)	0.75	0.02210	0.01007	0.01520	−0.00454	0.01704	−0.00058
Sc				0.25						
P1	0.0	0.0480(29)	0.0	0.5	0.04745	0.00717	0.04278	0.0	0.04496	0.0
Si1				0.5						
P2	0.3567(15)	0.1100(24)	0.2628(25)	0.5	0.04142	0.01432	0.02467	−0.00197	0.02833	0.00702
Si2				0.5						
O1	0.1468(30)	0.4403(30)	0.2130(43)	1.0	2.10					
O2	0.4366(24)	0.4484(28)	0.0856(31)	1.0	2.10					
O3	0.2536(19)	0.1852(42)	0.2076(44)	1.0	2.10					
O4	0.3781(31)	0.1342(38)	0.1199(41)	1.0	2.10					
O5	0.4484(19)	0.1813(42)	0.4258(39)	1.0	2.10					
O6	0.0783(24)	0.1462(33)	0.2362(43)	1.0	2.10					
Na1	0.25	0.25	0.5	0.69	0.13997	0.20638	0.09225	0.12141	0.05481	0.03729
Na2	0.50	0.9081(80)	0.25	0.86	0.05518	0.02554	0.16045	0.0	0.08663	0.0
Na3	0.8186(45)	0.0935(82)	0.8207(85)	0.73	0.06276	0.11943	0.16934	0.01690	0.04683	0.01757

crystal study carried out at elevated temperature (495K).

The Na2 coordination is more complicated as shown in Fig. 7. There are eight oxygens at distances of 2.43 to 2.94 Å forming an irregular polyhedron. Schioler (7) included two more oxygens in the coordination sphere at distances of 3.22 Å while Tranqui et al. (27) excluded these oxygens.

In the case of the monoclinic structure the Na1 sites are even more severely underoccupied than in the rhombohedral structure. In fact not one of the sodium sites is completely filled. If we consider only the Na–O interatomic distances that are less than 3.0 Å, then the coordination polyhedra are very similar to those reported by others (2, 7). They can be represented (Figs. 8 and 9) as a trigonal antiprism for Na1, a highly distorted trigonal prism
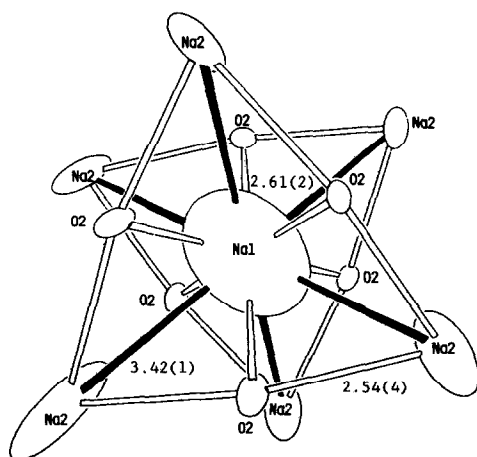

FIG. 6. An ORTEP representation of the coordination about Na1 in the rhombohedral $Na_3ScZrSiP_2O_{12}$ structure. Thermal ellipsoids are at the 20% probability level.

TABLE VII

Crystal Structure Data for Scandium-Substituted NASICONs; Bond Lengths and Angles for Monoclinic $Na_3Zr_{1.5}Sc_{0.5}P_{1.5}Si_{1.5}O_{12}$

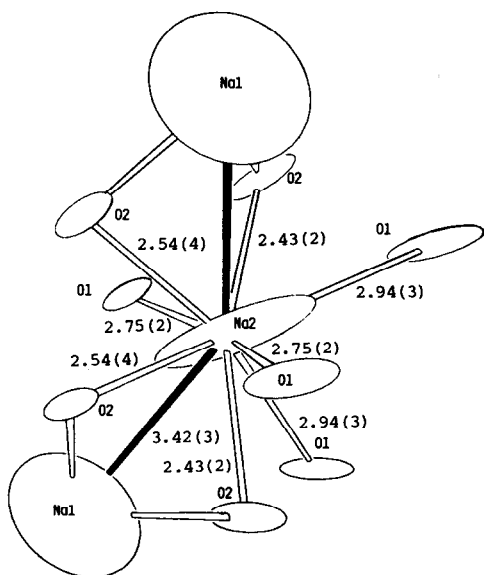| Atom	Bond length (Å)	Bond angle (deg)
Zr–O (ave)	2.087(6)	
Range	2.063–2.103	
$\begin{cases} P–O \\ Si–O \end{cases}$ (ave)	1.550(6)	
Range	1.521–1.571	
O–Zr–O (ave)		90.0(9)
O–P–O (ave)		109.4(9)
Zr–O–P (ave)		153(3)
Na1–O	2.585–2.783	Distorted O_h
Na1–Na3	2.79	
Na2–O	2.515–2.737	Distorted O_h
Na3–O	2.213–2.912	Distorted O_h

FIG. 7. An ORTEP representation of the coordination about Na2 in the rhombohedral $Na_3ScZrSiP_2O_{12}$ structure. Thermal ellipsoids are at the 20% probability level.

for Na3 and an irregular 8-fold coordination for Na2. All the sodium atoms are vibrating anisotropically with very large temperature factors.

Discussion

A very significant fact arising from this study is that no difficulty was experienced
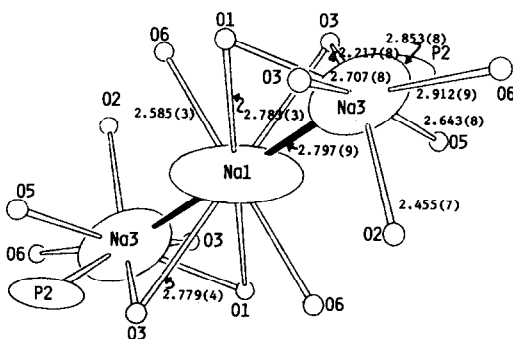

FIG. 8. An ORTEP representation of the coordination about Na1 and Na3 in the monoclinic $Na_3Sc_{0.5}Zr_{1.5}$ $Si_{1.5}P_{1.5}O_{12}$ structure. Thermal ellipsoids are at the 20% probability level. Oxygen atoms were not refined anisotropically.

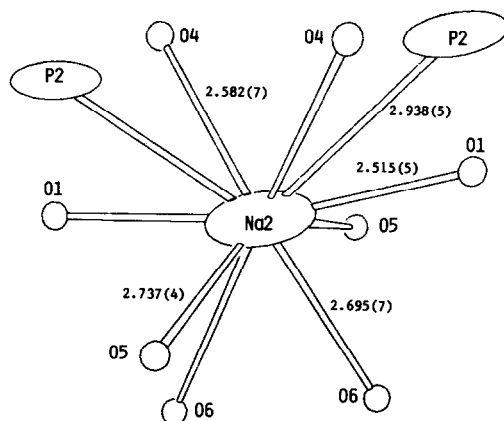FIG. 9. An ORTEP representation of the coordination about Na2 in the monoclinic $Na_3Sc_{0.5}Zr_{1.5}Si_{1.5}P_{1.5}$ O_{12} structure. Thermal ellipsoids are at the 20% probability level. Oxygen atoms were not refined anisotropically.

in preparing the compositions listed in Table I by high-temperature solid-state reactions. Refinement of occupancy factors for the two phases whose X-ray structures were determined confirmed their stoichiometries and rule out the presence of amorphous or glassy phases. The X-ray stoichiometries were the same as the ratios in the reactant mixes. This information needs to be considered in the light of a companion neutron diffraction study (28) on our hydrothermally prepared NASICON. In the hydrothermal preparation the stoichiometry arising from the refinement was $Na_{3.20}Zr_{1.68}Si_{1.84}P_{1.16}O_{11.54}$. The stoichiometry based upon analysis was $Na_{3.3}Zr_{1.65}Si_{1.9}$ $P_{1.1}O_{11.5}$ (9). However, the major reason for the low zirconium content is that about 0.3 mole of Na^+ was found in the zirconium positions. This was deduced from the fact that only 2.76 Na were found in the regular sodium positions and that the refinement would only converge when a partial Na^+ contribution in the Zr sites was included. The zirconium site occupancy could be completely accounted for as 1.66 Zr + 0.3 Na ≈ 2.0.

Kohler and Schulz (*13*) prepared single crystals from which they deduced a stoichiometry of $Na_{3.1}Zr_{1.78}Si_{1.24}P_{1.76}O_{12}$ based upon X-ray refinement and the requirements of charge balance. On this basis they suggested that the correct formulation for the NASICON solid solution is

$$Na_{1+x+4y}Zr_{2-y}Si_xP_{3-x}O_{12}. \qquad (2)$$
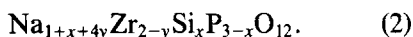
However, they found that the sodium sites were underoccupied and the observed (SiP)–O bond distance required x to be close to 2. The monoclinic structure of their crystals would also indicate that x is greater than 1.24; at least $x = 1.6$ is required to achieve the monoclinic structure (*7*). We would suggest that 0.22 Na^+ are located in the Zr sites accompanied by some oxygen deficiency to account for underoccupancy of the Na^+ sites and a higher silicon content.

The partial replacement of Zr^{4+} by Na^+ provides an explanation as to why other workers find it difficult to prepare the stoichiometric NASICON phase $Na_3Zr_2Si_2PO_{12}$. In the high-temperature solid-state reaction a stoichiometric amount of ZrO_2 is used. For each Na^+ ion in a Zr^{4+} site one ZrO_2 remains unreacted. Regrinding and reheating the mix results in very slow incorporation of the free ZrO_2, probably by replacement of Na^+ from the zirconium sites. This is a very slow reaction (and goes to completion with difficulty). It is now clear why such is the case, as the displacement of sodium in a very tightly bound octahedral environment by zirconium is expected to occur slowly and with a large energy barrier.

Since the amount of sodium replacing zirconium could vary dependent upon experimental conditions, there is no simple stoichiometric formula which can be utilized to represent NASICON compositions and those that have been proposed (*6, 13*) need to be carefully reexamined in the light of our structural results.

It would appear that the stoichiometric compositions observed in the scandium-substituted NASICONs results from the Sc^{3+} occupying Zr^{4+} sites and effectively excluding Na^+ from doing so. This point requires further investigation but indicates that NASICON synthesis is path dependent.

Another fact which should not be overlooked is that the structure for the monoclinic phase put forth by Hong (*2*) is correct in its essential features, even for the nonstoichiometric phases. However, in both the stoichiometric and nonstoichiometric phases it is clear that underoccupancy of the Na1 sites, as observed in this study and elsewhere (*7, 13*), is common. The sodium, where present in amounts of more than 1 mole, tends to distribute itself rather evenly over the available sites. Further we might expect that the Na^+ ions in the zirconium sites are nonconducting. Our thermal parameters for Na1 in the rhombohedral phase are very similar to those obtained by Tranqui *et al.* (*27*) for a single crystal study of $Na_4Zr_2Si_3O_{12}$ while those for Na2 are about twice the values given by Tranqui. This similarity occurs even though only three-fourths of the cavities are filled in our scandium-substituted phase as opposed to all the cavities being filled in the Na_4 compound. Thus one might conclude, albeit guardedly, that the conduction pathway is similar; that is, Na2 to Na2 in the rhombohedral phase. However, in the monoclinic phase it appears that a more complex pathway involving all three sodium ion sites is possible. This may account for the larger room temperature conductivity of the monoclinic phases relative to the rhombohedral ones even though they contain the same number of sodium ions. In order to answer some of these questions we have undertaken a detailed neutron diffraction study as a function of temperature of the two phase types.

Acknowledgment

References

1. J. B. Goodenough, H. Y.-P. Hong, and J. A. Kafalas, *Mater. Res. Bull.* **11,** 204 (1976).
2. H. Y.-P. Hong, *Mater. Res. Bull.* **11,** 173 (1976).
3. M. L. Bayard and G. G. Barna, *J. Electroanal. Chem.* **91,** 201 (1978).
4. J. P. Boilot, J. P. Salanie, G. Desplances, and D. Le Potier, *Mater. Res. Bull.* **14,** 1469 (1979).
5. R. S. Gordon, G. R. Miller, B. J. McEntire, E. D. Beck, and J. R. Rasmussen, *Solid State Ionics* **3/4,** 243 (1981).
6. U. von Alpen, M. F. Bell, and H. H. Hoefer, *Solid State Ionics* **3/4,** 214 (1981).
7. L. J. Schioler, Ph.D. dissertation, Mass. Inst. Technol., Feb. 1983.
8. A. Clearfield, P. Jerus, and R. N. Cotman, *Solid State Ionics* **5,** 301 (1981).
9. A. Clearfield, M. A. Subramanian, W. Wang, and P. Jerus, *Solid State Ionics* **9/10,** 895 (1983).
10. J. Engell, S. Mortenson, and L. Moller, *Solid State Ionics* **9/10,** 877 (1983).
11. A. Clearfield, *Solid State Ionics* **9/10,** 823 (1983).
12. H. Kohler, H. Schulz, and O. Melnikov, *Mater. Res. Bull.* **18,** 589 (1983).
13. H. Kohler and H. Schulz, *Solid State Ionics* **9/10,** 795 (1983).
14. A. Clearfield and S. P. Pack, *J. Inorg. Nucl. Chem.* **13,** 2880 (1974).
15. "LSUCRE, Program for Least-Squares Unit Cell Refinement," Univ. Freiburg (1972). Modified by P. R. Rudolf, Texas A&M University (1982).
16. W. I. Archer and R. D. Armstrong, "Electrochemistry," Vol. 7, Chapt. 3 (Chem. Soc.), Alden Press, London (1980).
17. K. Frase, Ph.D. dissertation, Univ. Pennsylvania (1983).
18. P. R. Rudolf and A. Clearfield, *Acta Crystallogr.* **B,** in press.
19. Ch. Baerlocher and A. Hepp, "The X-Ray Rietveld System," Institut fuer Krist. und Petrographie, ETH, Zurich (1982).
20. H. Y.-P. Hong, J. A. Kafalas, and M. Bayard, *Mater. Res. Bull.* **13,** 757 (1978).
21. D. Y. Wang and A. S. Nowick, *J. Solid State Chem.* **35,** 325 (1980).
22. M. Kleitz and J. H. Kennedy, "Fast Ion Transport in Solids" (P. Vashishta, J. N. Mundy, and G. K. Shenoy, Eds.), p. 185, North–Holland (1979).
23. U. von Alpen, M. F. Bell, and W. Wichelhaus, *Mater. Res. Bull.* **14,** 1317 (1979).
24. C. K. Johnson, Report ORNL-3794; Oak Ridge National Laboratory: Oak Ridge, Tenn. (1965).
25. L. Hagman and P. Kierkegaard, *Acta Chem. Scand.* **22,** 1822 (1968).
26. R. G. Sizova, A. A. Voronkov, N. G. Shumatskaya, V. V. Ilyukhin, and N. V. Belov, *Sov. Phys. Dokl.* **17,** 618 (1973).
27. D. Tranqui, J. J. Caponi, J. C. Joubert, R. D. Shannon, and C. K. Johnson, *in* "Fast Ion Transport in Solids," Proc. Int. Conf., Lake Geneva, Wisc., May 1979, p. 439, Elsevier/North–Holland, New York (1979).
28. P. R. Rudolf, M. A. Subramanian, A. Clearfield, and J. D. Jorgensen, *Mater. Res. Bull.* **20,** 643 (1985).